

# Charge Symmetry Breaking in the Valence Quark Distributions of the Nucleon

C.J. Benesh<sup>1,2,3</sup> and T. Goldman<sup>1</sup>,

1-Los Alamos National Laboratory, Los Alamos, NM 87545,

2-International Institute for Theoretical and Applied Physics,  
Iowa State University, Ames, Iowa 50010,

3-Current Address: Nuclear Theory Center, Indiana University,  
Bloomington, IN 47408.

June 16, 2021

## Abstract

Using a quark model, we study the effect of charge symmetry breaking on the valence quark distributions of the nucleon. The effect due to quark mass differences and the Coulomb interaction of the electrically charged quarks is calculated and, in contrast to recent claims, found to be small. In addition, we investigate the effect of charge symmetry breaking in the confining interaction, and in the perturbative evolution equations used to relate the quark model distributions to experiment. We find that both these effects are small, and that the strong charge symmetry breaking effect included in the scalar confining interactions may be distinguishable from that generated by quark mass differences.

# 1 Introduction

The study of charge symmetry and its breaking is almost as old as nuclear physics itself. From the earliest days of isospin[1], to modern attempts to understand small effects in the nucleon-nucleon interaction[2], the study of this symmetry has provided a rare window into the non-perturbative dynamics of low energy hadronic phenomena. The interactions responsible for charge symmetry breaking (CSB) are largely understood and relatively weak, so that the study of CSB provides a sensitive filter with which to test the hadronic wavefunctions of nuclei and nucleons. In the case of QCD, where the interactions that bind quarks into hadrons are only understood schematically and the theoretical landscape is cluttered with different phenomenological models, such probes may prove especially valuable.

In this paper, we study the effect of the breaking of charge symmetry on the valence quark distributions of the nucleon. Our interest in this topic is generated by the observation of unexpected effects in both the sea[3] and spin-dependent[4] quark distributions of the nucleon, and by the possibility that large CSB effects in the valence distributions of the nucleon may play a non-negligible role in the extraction of  $\sin^2 \theta_W$  from  $\nu - N$  data[5]. Recent calculations have claimed that charge symmetry breaking may be greatly enhanced by kinematic effects associated with diquarks in the nucleon wavefunction[6], and that the resulting CSB may be large enough to be observed directly. Our calculations provide an important check on the model dependence of these results, as well as investigating several sources of CSB not considered in Ref. 6.

The paper is structured as follows: In Section 2, the method we use to extract quark distributions from quark models is reviewed, with particular emphasis on those details of the calculation that will be affected by charge symmetry breaking. In the next section, the shift in the valence quark distributions due to the breaking of charge symmetry by quark masses, and by Coulomb effects is calculated for both the minority and majority quark distributions in the nucleon. The effect of the difference between the neutron and proton mass is also discussed and, after concluding that it contains no physics, discarded. The fourth section is devoted to a discussion of the possibility of charge symmetry breaking in the confining interaction itself, and the possibility that such effects may be distinguishable from ordinary quark mass effects on the valence distributions, while in the fifth we calculate the charge symmetry breaking effect due to the perturbative evolution of the valence distributions that is required if the quark model is to make contact with high energy data. The final section compares our results to those of references 5 and 6, and discusses the prospects for measuring CSB in the valence distributions directly.

## 2 Valence Quark Distributions in the Los Alamos Model Potential (LAMP).

Quark models were originally constructed to provide a description of low energy hadronic data using only effective interactions between valence quarks. In order to make sensible

calculations of valence quark distributions, the stark simplicity of quark models must be reconciled with the richer vision afforded by data from higher energies, where nucleons are composed not only of valence quarks, but also of sea quarks and gluons. Remarkably, these two very different pictures may be accommodated by QCD via the renormalization group[7]. Quark models may be interpreted as representations of QCD at an intermediate renormalization scale,  $\mu_{QM}^2$ , large enough so that the quark substructure of the nucleon is revealed, but small enough that the sea quarks and glue are almost entirely absorbed by a redefinition of the valence quarks. Parton distributions at this intermediate scale may be calculated in terms of the quark model, and then evolved to higher energies using perturbative QCD[8] and compared to data.

The first step in this procedure is to calculate the quark distributions at the quark model scale. For unpolarized scattering, the relevant matrix elements are given by[8]

$$\begin{aligned} q_i(x) &= \frac{1}{4\pi} \int d\xi^- e^{iq^+\xi^-} \langle N | \bar{\psi}_i(\xi^-) \gamma^+ \psi_i(0) | N \rangle |_{LC} \\ \bar{q}_i(x) &= -\frac{1}{4\pi} \int d\xi^- e^{iq^+\xi^-} \langle N | \bar{\psi}_i(0) \gamma^+ \psi_i(\xi^-) | N \rangle |_{LC}, \end{aligned} \quad (1)$$

where  $q^+ = -Mx/\sqrt{2}$  (with  $x \equiv x_{Bj}$  the Bjorken scaling variable),  $\psi_i(\bar{\psi}_i)$  are field operators for quarks of flavor  $i$ ,  $\gamma^+$  is a Dirac gamma matrix, and the subscript LC indicates a light cone condition on  $\xi$ , namely that  $\xi^+ = \vec{\xi}_\perp = 0$ .

For a given model, valence quark distributions can be obtained via a number of different prescriptions that have arisen in the literature[9, 10, 11]. The approach we adopt consists of a straightforward evaluation of the matrix elements of Eq. 1 in a Peierls-Yoccoz projected momentum eigenstate, assuming that the time dependence of the field operator is dominated by the lowest eigenvalue of the Dirac equation used to obtain the wavefunctions of the struck quark. The details of this procedure are described in Ref. 9, where the valence quark distributions are shown to be given by

$$xq_V^i(x) = \frac{MxN_i}{\pi V} \left\{ \left[ \int_{|k_-|}^{\infty} dk G_i(k) \left( t_{i0}^2(k) + t_{i1}^2(k) + 2\frac{k_-}{k} t_{i0}(k)t_{i1}(k) \right) \right] + [k_- \rightarrow k_+] \right\}, \quad (2)$$

where

$$\begin{aligned} G_i(k) &= \int r dr \sin kr \Delta_{s1}(r) \Delta_{s2}(r) EB(r), \\ V &= \int r^2 dr \Delta_i(r) \Delta_{s1}(r) \Delta_{s2}(r) EB(r), \\ t_{\alpha 0}(k) &= \int r^2 dr j_0(kr) u_\alpha(r), \\ t_{\alpha 1}(k) &= \int r^2 dr j_1(kr) v_\alpha(r), \\ \Delta_\alpha(r) &= \int d^3z \phi_{0\alpha}^\dagger(\mathbf{z} - \mathbf{r}) \phi_{0\alpha}(\mathbf{r}), \end{aligned} \quad (3)$$

with  $\phi_{0\alpha}(\mathbf{r})$  the ground state valence quark wavefunction for a quark of flavor  $\alpha$ , with upper and lower components  $u_\alpha(r)$  and  $i\sigma \cdot \mathbf{r}v_\alpha(r)/r$ ,  $k_\pm = \omega_i \pm Mx$ , with  $\omega_i$  the ground state

struck quark energy eigenvalue,  $EB(r) = \langle EB, \mathbf{R}_{\text{CM}} = \mathbf{r} | EB, \mathbf{R}_{\text{CM}} = \mathbf{0} \rangle$  is the overlap function for two “empty bags” separated by a distance  $r$ , which accounts for the dynamics of the confining degrees of freedom. Finally, the subscripts  $s1$  and  $s2$  denote the flavor of the two spectator valence quarks that make up the nucleon.

All calculations described in this paper are carried out using the Los Alamos Model Potential (LAMP)[12], in which valence quarks are confined by a linear potential of the form

$$V(r) = \beta k(r - r_0) \quad (4)$$

with parameters  $k=0.9$  GeV and  $r_0=0.57$  fm chosen to reproduce the average nucleon-delta mass, and  $\beta$  is a Dirac gamma matrix. We further assume that the function  $EB(r)$  is a constant[13], and unless otherwise noted, quarks are taken to be massless.

### 3 Charge Symmetry Breaking

As we have already noted, the sources of charge symmetry breaking are light quark mass differences and the electro-magnetic interaction. CSB effects may be manifested either directly, as a result of explicit mass or interaction terms in the quark model hamiltonian, or indirectly as a result of mixing between the symmetry violating terms and the strong interaction. In this section, we calculate the direct terms, deferring discussion of the numerically smaller mixed interactions for later.

At the partonic level, charge symmetry predicts that the u quark distribution in the proton is equal to the d quark distribution in the neutron, with a corresponding prediction for the d distribution. A measure of the extent to which the symmetry is broken is given by the ratios

$$\begin{aligned} R_{CSB}^{maj}(x) &= \frac{2[u_V^p(x) - d_V^n(x)]}{[u_V^p(x) + d_V^n(x)]} \\ R_{CSB}^{min}(x) &= \frac{2[d_V^p(x) - u_V^n(x)]}{[d_V^p(x) + u_V^n(x)]}, \end{aligned} \quad (5)$$

where  $u(d)_V^{p(n)}(x)$  denotes the up(down) valence quark distribution in the proton(neutron).

#### 3.1 CSB in Quark Wavefunctions

The simplest mechanism for altering the shape of the valence distributions of the nucleon in Eq. 2 is to change the model wavefunctions for the struck and spectator quarks. Since these wavefunctions are generated by solving a Dirac equation in the mean confining field of the other quarks, direct CSB effects may be included without additional assumption by including appropriate terms in the Dirac Hamiltonian.

We have recalculated the valence quark wavefunctions assuming quark masses  $m_u = 4$  MeV and  $m_d = 8$  MeV[14]. In Figs. 1 and 2, the CSB ratios produced by these wavefunctions are indicated by the dashed curves. For minority quarks, the ratio starts small and rises to

+1.5% at large  $x$ , while the majority quark ratio rises more slowly, but is still positive. The fact that these ratios are of the same sign and comparable in magnitude may be understood, since, when the struck quark is a majority quark, the two spectators are in a charge symmetric state. The only change is due to the change in the valence quark wavefunction. When a minority quark is struck, the change in the wavefunction of the struck quark is compensated for by the change in the wavefunctions of the two spectators, which alter the momentum projection factor  $G_i(k)$  in Eq. 1, and are of opposite sign and roughly twice as large as the effect produced by the struck quark wavefunction.

In addition, we have calculated the effect of the Coulomb interaction between the charged quarks using a mean field approximation for the electric potential between a quark of charge  $q$  and the other valence quarks, given by

$$V_{Coul}(r) = \alpha q(Q_N - q) \int d^3r' \frac{\phi^\dagger(r')\phi(r')}{|\mathbf{r} - \mathbf{r}'|}, \quad (6)$$

where  $Q_N$  is the charge of the nucleon being studied. The CSB contribution generated by the Coulomb effect on the quark wavefunctions is shown by the dot-dashed curves in Figs. 1 and 2. Again, the CSB effect produced by perturbing the wavefunctions is significantly smaller for the minority quark distributions. In this instance, the change in the wavefunction due to the Coulomb force is, to first order in  $\alpha$ , the same for either minority quark. Even for the majority quarks, the Coulomb correction is much smaller than 1%. Magnetic corrections have not been calculated explicitly, but since they are similar in structure to the color magnetic corrections responsible for breaking SU(4) symmetry in the quark distributions[9], yet are suppressed relative to those corrections by both the smallness of the electromagnetic coupling constant and by color SU(3) factors, their effect should also be very small.

### 3.2 CSB in the Dirac Eigenvalue

Along with the wavefunctions, solution of Dirac equation provides an energy eigenvalue which determines the time dependence of the lowest mode of the confined quark field. This energy is just that required to break the bonds which tie the struck quark to the spectators, and as such is sensitive to the nature of the interactions that bind the quarks together. Since the dependence of the quark distribution functions on this eigenvalue has the same functional form regardless of whether the changes in the eigenvalue are produced by quark mass effects or Coulomb interactions, we have simply taken the changes in the eigenvalues produced by the Hamiltonian changes already described and added them together. For the proton the quark eigenvalues were shifted from the value for massless quarks (361.8 MeV) to  $\omega_u = 364.2$  MeV and  $\omega_d = 365.0$  MeV. The corresponding values for the neutron are  $\omega_u = 363.0$  MeV and  $\omega_d = 365.6$  MeV. The CSB ratios obtained using these eigenvalues, and massless quark wavefunctions, are shown by the solid lines in Figs. 1 and 2. At large  $x$ , these shifts produce CSB effects on the order of 2-3%, which, may be understood from Eq. 1 as the fractional shift in the quark eigenvalue enhanced by the slope of the unperturbed quark distribution. (This is the closest analog to the diquark mass shift of Ref. 6, and correspondingly produces the largest effect.)

### 3.3 Proton-Neutron Mass Difference

The results of changing the nucleon mass parameter appearing in Eq. 1 to reflect the difference in mass of the proton and neutron is shown by the dotted curves in Figs. 1 and 2. Like the quark eigenvalue, the effect of changing the nucleon mass parameter is enhanced, at large  $x_{Bj}$ , by the slope of the unperturbed quark distribution function.

This effect, however, will not be present if the data is analyzed in the conventional manner because the nucleon mass appears not only as an explicit parameter in Eq. 1, but is also implicit in the definition of  $x_{Bj}$  (In deep inelastic lepton production, for example,  $x_{Bj} = Q^2/2M_{nuc}q_0$  in the target rest frame.). In fact, the combination  $M_{nuc}x_{Bj}$ , which is all that appears in Eq. 2 for  $xq(x)$ , is completely independent of  $M_{nuc}$ ! This is in accord with what one would expect in a light cone formalism, where  $P^+$  is a kinematical variable, and therefore immune to the dynamical effects which violate charge symmetry. (While it is certainly possible to alter the usual analysis by rescaling  $x_{Bj}$  once the neutron structure function is extracted from the raw data, it not clear what would be learned by comparing the probability of finding quarks in the proton at one momentum to that in the neutron at a slightly different momentum.) Hence, we assert that there is no CSB effect in the parton distributions due to the neutron-proton mass difference[15].

## 4 CSB in the Confining Interaction

The existence of CSB interactions induced by mixing the electromagnetic and strong couplings was first pointed out in Ref. 16, where it was argued that the quark-gluon vertex picks up a charge asymmetric contribution from photon loops[16]. Since the confining potential must, at some level, be composed of multiple gluon exchanges[17], the existence of this coupling implies that the confining potential will not be charge symmetric. Unfortunately, since the confining potential is a Lorentz scalar, the CSB contribution to the energy of light quark hadrons is indistinguishable from the effect of quark mass differences.

In this section, we examine the possibility of distinguishing CSB in the confining potential from quark mass effects by looking at the relative contribution of each to CSB in the valence quark distribution. Since there is, at present, no means to calculate the confining potential, nor its correction due to charge symmetry violation, we proceed to model the effect by altering the string tension parameter used in the LAMP model potential. Furthermore, since the relative normalization of the two effects is unknown, we proceed by arbitrarily normalizing the shift in the string tension such that it produces the same first order shift in the quark eigenvalue as the corresponding quark mass. The wavefunctions that result from this change are then used in Eq. 1 to produce the the charge symmetry breaking ratios shown in Fig. 3. The solid and short-dashed curves indicate the CSB ratios for majority and minority quarks produced by a 4 MeV quark mass difference, while the long-dashed and dot-dashed curves are the same ratios produced by the change in the string tension. Significantly, the CSB produced by the change in the string tension has the opposite sign to that produced by quark mass differences, opening the possibility that the two effects may

be distinguished from one another by precise measurement of CSB in the valence quark distributions.

## 5 Evolution

Having separated out the CSB effects at a low momentum scale, we must now evolve to high  $Q^2$  so that a comparison with data is possible. Two issues arise: First, does the perturbative evolution erase the CSB effects we have calculated, and secondly, how large are the CSB effects in the evolution itself?

In Figs. 4 and 5, we show the results obtained by evolving both the CSB pieces of the valence quark distributions and the symmetric distributions from a low quark model scale, taken to be  $0.5 \text{ GeV}^2$ , to  $10 \text{ GeV}^2$ [8]. For both majority and minority quarks the evolution has only a small effect on the CSB ratios, shifting the curves to low  $x$  and slightly increasing the magnitude of the ratio.

Also shown in Figs. 4 and 5 is the contribution to the CSB ratio provided by charge symmetry breaking effects generated when a quark splits into a quark and a photon[18]. To leading order in  $\alpha$ , the structure of the QED and QCD contributions to the evolution differ only by constant factors, and the effect of including the photon diagram is to slightly speed up the rate at which the valence distributions evolve. Since the coupling of the photon is charge asymmetric, this means that the  $u$  distribution evolves slightly faster than the  $d$  distribution. As shown in the figures, this effect is larger than the effect of Coulomb repulsion in the quark wavefunctions, but is nonetheless still quite small.

## 6 Comparison and Experimental Prospects

In Ref. 6, the effect of charge symmetry violation on the valence quark distributions was calculated via the introduction of an intermediate state diquark. The resulting two-body kinematics produces an additional enhancement of the CSB effect produced by small changes in the diquark mass, resulting in a 5-10% CSB ratio for minority quarks in the range  $0.5 < x < 0.7$ , roughly twice the size of our result. For majority quarks, the two calculations are comparable. In reference 5, using a model independent approach, Sather obtains slightly smaller ratios for the majority quarks than in this work, and similar results for the minority quarks. Generally, each of these calculations predict larger CSB effects in the minority quark distributions than in the majority distributions.

Experimentally, the situation is less clear. As pointed out in Ref. 18, measurements of CSB generally yield not the ratios for the majority/minority quarks separately, but rather the ratio for the entire valence distribution, given by

$$R_{val} = \frac{2 [d_V^p(x) - u_V^p(x) - u_V^n(x) + d_V^n(x)]}{[u_V^p(x) + d_V^p(x) + u_V^n(x) + d_V^n(x)]}. \quad (7)$$

Since the minority quark distribution is suppressed at large  $x_{Bj}$  by SU(6) symmetry breaking effects[20], the ratio is less sensitive to the (fractionally) larger charge symmetry breaking in the minority distribution, which is the major difference between the models. While it is possible to isolate the minority distribution by comparing  $\pi^+ - p$  and  $\pi^- - D$  Drell-Yan cross sections[19], the systematic errors associated with beam normalizations and the deuteron EMC effect will make it difficult to unambiguously separate the small effects predicted in this work.

Regardless of the result, the information provided by these experiments will provide new insights into the soft dynamics of quarks in the nucleon, and possibly a means to distinguish experimentally between CSB generated by quark mass differences and the mixing of the strong and electro-magnetic interactions.

### Acknowledgments

The work of C.B. and T.G. was performed under the auspices of the U.S. Department of Energy. One of us (C.B.) gratefully acknowledges the support of the Iowa Space Grant Cooperative and the hospitality of the Physics Department of the Univ. of Northern Iowa during the final stages of this work.

## References

- [1] W. Heisenberg, Z. Phys. 77, 1(1932).
- [2] G. A. Miller and W.T.H. van Oers, in *Symmetries and Fundamental Interactions in Nuclei*, eds. W. Haxton and E. Henley, World Scientific. (Singapore) 1996, G.A. Miller, B. Nefkens, and I. Slaus, Phys. Rep. 194, 1(1990).
- [3] New Muon Collaboration, Nucl. Phys. **A577**, 325(1994); Phys. Rev. **D50**, 1(1994); Phys. Rev. Lett. **66**, 2712(1991).
- [4] J. Ashman et. al., Phys. Lett. **B206**, 3641(1988); Nucl. Phys. **A328**, 1(1988), Spin Muon Collaboration, Nucl. Phys. **A577**, 313(1994); Phys. Lett. **B320**, 400(1994); Phys. Lett. **B329**, 399(1994); Phys. Lett. **B357**, 248(1995), P.L. Anthony et. al., Phys. Rev. Lett. 71, 959(1993), K. Abe et. al., Phys. Rev. Lett. 74, 346(1995).
- [5] E. Sather, Phys. Lett. **B274**, 433(1992).
- [6] E. Rodionov, A. W. Thomas and J. T. Londergan, Int. J. Mod. Phys. **A9**, 1799(1994).
- [7] R. L. Jaffe and G. G. Ross, Phys. Lett. **93B**, 313(1980).
- [8] C.J. Benesh, Mod. Phys. Lett. **A9**, 849(1992), S. Kumano, J.T. Londergan, Comput. Phys. Commun. **69**, 373(1992), M. Miyama and S. Kumano, SAGA preprint SAGA-HE-81-95, hep-ph 9508246,

- R. Kobayashi, M. Konuma, S. Kumano, M. Miyama, Prog. Theor. Phys. Supp. **120**, 257(1995).
- [9] C. J. Benesh and G.A. Miller, Phys. Rev. **D36**, 1344 (1987); Phys. Rev. **D38**, 48(1988); Phys. Lett. **B215**, 381(1988).
- [10] A. J. Signal and A. W. Thomas, Phys. Rev. **D40**, 2832(1989); A. W. Thomas, Nucl. Phys. **A532**, 177c(1991).
- [11] X.M. Wang and X. Song, Phys. Rev. **C51**, 2750(1995),  
W. Melnitchouk and W. Weise, Phys. Lett. **B334**, 275(1994),  
K. Suzuki, T. Shigetani, and H. Toki, Nucl. Phys. **A573**, 541(1994),  
F. Gross and J. Milana, Phys. Rev. **D43**, 2401(1991),  
V. SanJose and V. Vento, Nucl. Phys. **A501**, 672(1989).
- [12] T. Goldman, K.R. Maltman, G.J. Stephenson Jr., and K.E. Schmidt, Nucl. Phys. **A481**, 621(1988).
- [13] Relaxing this assumption will produce quarks distributions that are larger at small  $x$  and at large  $x$ . Since we do not expect that the magnitude of the CSB effect will be sensitive to this assumption, the CSB ratios are expected to decrease for large and small  $x$ , and to increase in between.
- Constructing such an overlap for a linear confining potential, as opposed to a bag-like potential, may seem intractable due to infrared divergences. However, such a potential can be described as arising from a scalar field strength distribution that falls off Coulombically at large  $r$ . Since it is the field strength distribution, *not* the interaction energy, that is the appropriate object to appear in the empty bag overlap function, the infrared problems disappear. For a discussion of this see T. Goldman, ‘Confinement Unstrung’, to appear in the Proceedings of the Workshop “Quark Confinement and the Hadron Spectrum II”, Como, Italy, June 26-29, 1996, ed. by N. Brambilla, World Scientific.
- [14] R.P. Bickerstaff and A.W. Thomas, Phys. Rev. **D25**, 1869(1982).
- [15] The issue of the consistent definition of  $x_{Bj}$  is overlooked in both Refs. 5 and 6, leading to predictions for the CSB effect in the valence distributions which cannot, therefore, be correct. In Ref. 6, there is a legitimate effect due to the additional kinematic role played by the nucleon mass, but, as discussed in the text, such effects are in disagreement with the expectations of light cone physics. We conclude that they are artifacts of the diquark approximation used to completely specify the model kinematics.
- [16] T. Goldman, K.R. Maltman, and G.J. Stephenson Jr., Phys. Lett. **B228**, 396(1989).
- [17] See A.S. Goldhaber and T. Goldman, Phys. Lett. **B344**, 319(1995), for a detailed discussion of this point.

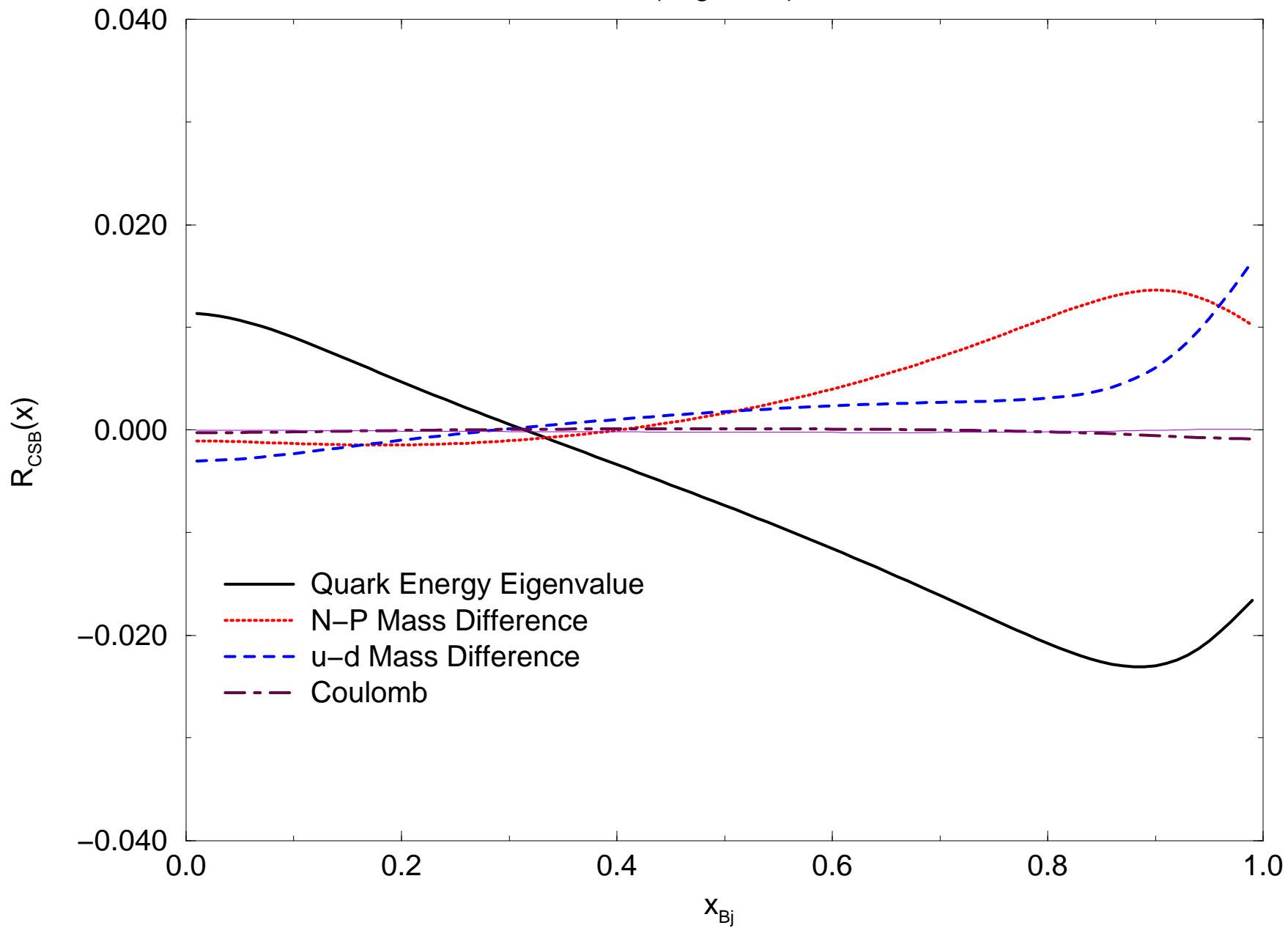
- [18] H. Spiesberger, Phys. Rev. **D52**, 4936(1995).
- [19] J.T. Londergan, G.T. Garvey, G.Q. Liu, E.N. Rodionov and A.W. Thomas, Phys. Lett. **B340**, 115(1994).
- [20] C. J. Benesh, T. Goldman, and G.J. Stephenson Jr., Phys. Rev. **C48**, 1379(1993),  
F.E. Close and A.W. Thomas, Phys. Lett. **B212**, 229(1988).

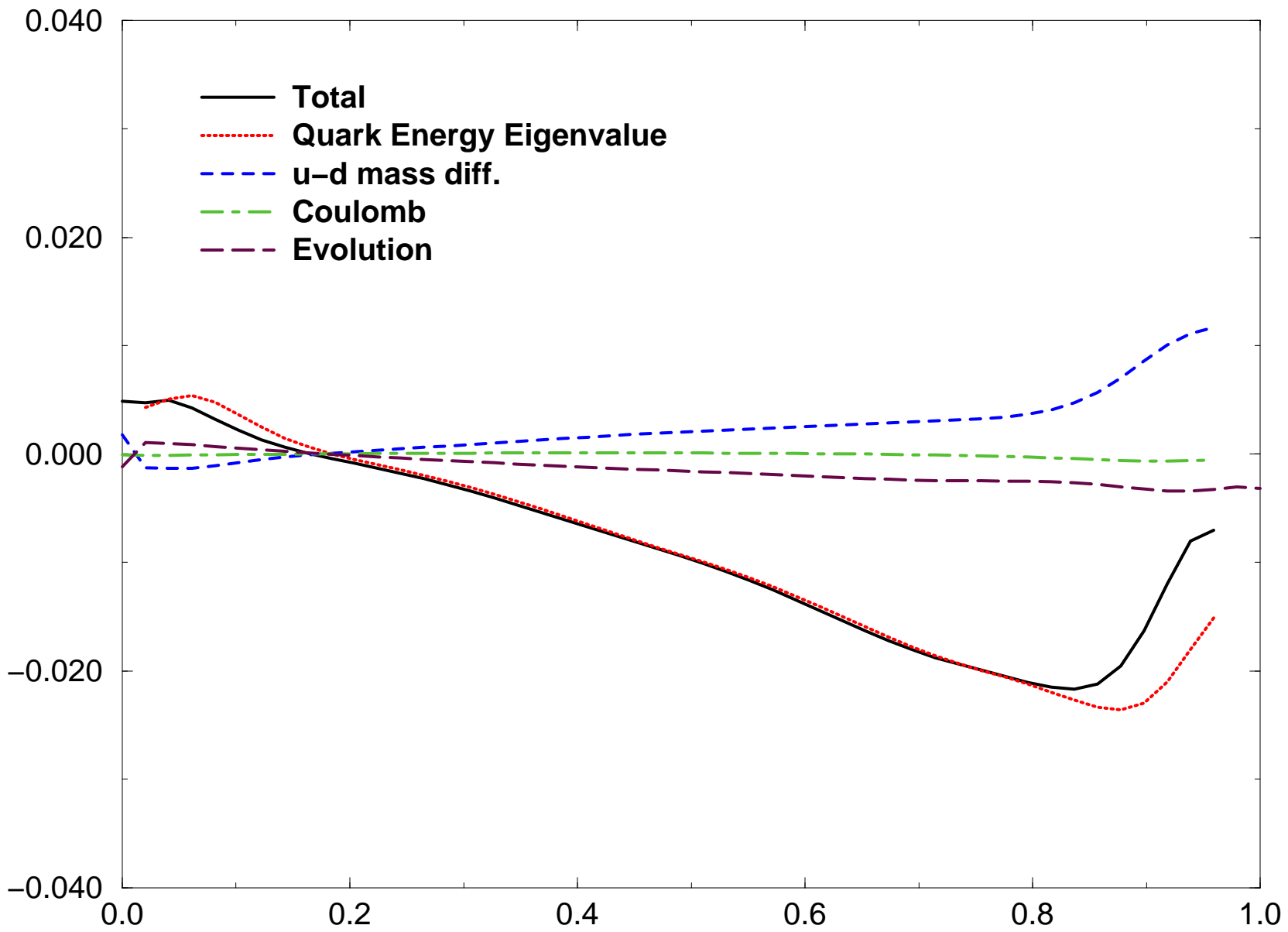
## Figure Captions

- Figure 1 - Charge Symmetry Ratio for Majority (valence) quarks in the nucleon at the quark model scale.
- Figure 2 - Charge Symmetry Ratio for minority (valence) quarks in the nucleon at the quark model scale.
- Figure 3 - Comparison of Charge Symmetry breaking produced by quark mass differences with that induced by mixing of the electro-magnetic and confining interactions.
- Figure 4 - Charge Symmetry Ratio for Majority (valence) quarks in the nucleon at a scale of  $10 \text{ GeV}^2$ . The sum of all contributions is shown by the solid line, while the other lines are described in the text.
- Figure 5 - Charge Symmetry Ratio for Minority (valence) quarks in the nucleon at a scale of  $10 \text{ GeV}^2$ . The sum of all contributions is shown by the solid line, while the other lines are described in the text.

# Majority Quark Ratio

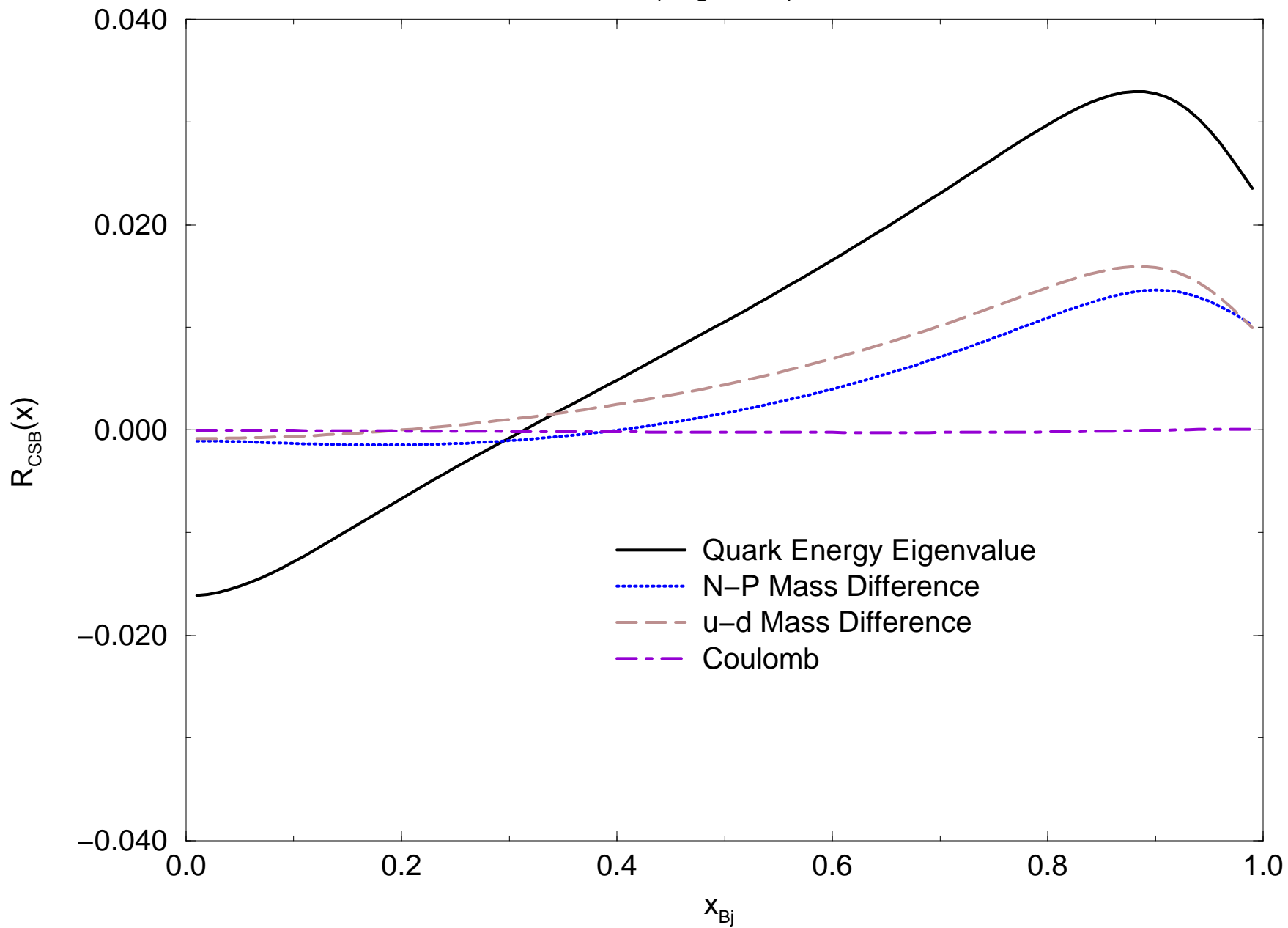
(bag scale)





# Minority Quark Ratio

(bag scale)



# Minority Quark Ratio

(10 GeV<sup>2</sup>)

